

Ion Acceleration and Coherent Structures Generated by Lower Hybrid Shear-Driven Instabilities

H. Romero and G. Ganguli

Space Plasma Branch, Plasma Physics Division, Naval Research Laboratory, Washington, D.C. 20375

Y. C. Lee

Department of Physics and Astronomy, University of Maryland, College Park, Maryland 20742

(Received 16 September 1992)

It is shown that if $\kappa = \omega_S / \omega_{LH} > 1$ (ω_S and ω_{LH} are the shear and lower hybrid frequencies), a sheared electron cross-field flow excites the electron-ion-hybrid mode, causing significant perpendicular ion acceleration. The electric potential develops coherent structures (vortexlike) longer than the electron Larmor radius, ρ_e . For $\kappa < 1$, a smooth transition occurs where the wavelength becomes of the order of ρ_e , the lower hybrid drift instability dominates, and the formation of vortexlike structures is no longer observed. The results are relevant to laboratory, laser-produced, and space plasmas.

PACS numbers: 52.35.Qz, 52.35.Ra, 52.65.+z, 94.30.Gm

In this Letter, we report several novel effects that arise in the nonlinear evolution of lower hybrid waves driven unstable by the presence of shear in an electron cross-field flow. We denote the flow's peak velocity by V_0 and the characteristic distance over which it is localized by L_E . The regime $\rho_e < L_E < \rho_i$ is considered, where ρ_e and ρ_i denote the electron and ion Larmor radii, respectively. Such flows are commonly encountered in laboratory and space plasmas; their occurrence plays an important role in the dynamical evolution of a variety of physical systems including the earth's magnetospheric boundary layers (such as the magnetopause or the plasma sheet boundary layer) [1], laser-produced plasmas [2], and chemical release experiments in the Earth's magnetotail [3].

It is well known that an electron cross-field flow can excite lower hybrid waves via the lower hybrid drift [4] or modified two-stream [5] instabilities. In this work, we show that when a sufficient amount of shear is present in the electron flow (as is the case in a number of realistic cases) significant modifications occur in the nonlinear state generated by these waves. To this end, we define the shear frequency $\omega_S = V_0 / L_E$. It is shown that if ω_S is comparable to or larger than the frequency of the wave of interest (in this work it is the lower hybrid frequency ω_{LH}), velocity shear leads not only to quantitative modifications of the nonlinear waves, but to the appearance of a new mode in the system that can dominate its dynamical evolution and significantly alter its final nonlinear state. We have recently reported the linear properties of this new plasma mode which we denote as the electron-ion-hybrid (EIH) instability [6].

The equilibrium configuration consists of an electron-ion plasma immersed in a uniform magnetic field that is directed along the z axis: $\mathbf{B} = B_0 \mathbf{a}_z$. A boundary layer of width L_E separates two regions, one containing a high-density plasma and the other a low-density plasma. To be specific, we assume that the density variation occurs along the x axis, i.e., in a direction perpendicular to the

confining magnetic field. In equilibrium, since $L_E < \rho_i$, no bulk ion motion occurs [6]. Ion force balance then requires the existence of a localized electric field, directed along the x axis, in order for this density gradient to be maintained. It is convenient to choose the spatial variation of the localized electric field in the range $0 < x < L_x$ as follows:

$$E(x) = (E_0 / N_0) \{F(\xi - x_0) - F(\xi + x_0)\}, \quad (1)$$

where

$$\xi = x - L_x / 2,$$

$$F(\zeta) = \text{sech}^2(\zeta / L_E),$$

$$N_0 = 1 - \text{sech}^2(2x_0 / L_E)$$

is a normalization constant, and x_0 determines the distance separating the two regions in which the externally imposed electric field is either positive or negative. In this paper, $x_0 \gg L_E$ which yields $N_0 \approx 1$. Then, the peak value of the electric field occurs at the points $L_x / 2 \mp x_0$ and is given by $\pm E_0$, respectively. Since the ion temperature T_i is assumed to be spatially uniform, force balance gives the following expression for the ion density: $n_i(x) = N_i \exp[(C_i / N_0) D(\xi)]$, where $C_i = 2E_0 L_E / B_0 \rho_i V_i$, V_i is the ion thermal velocity, N_i is a constant, $D(\xi) = G(\xi - x_0) - G(\xi + x_0)$, and $G(\zeta) = \tanh(\zeta / L_E)$. The resulting density profile is symmetric about the point $L_x / 2$, allowing the use of periodic boundary conditions in the numerical simulation of the time evolution of the system. Of course, in equilibrium, the ion velocities are given by an isotropic nondrifting Maxwellian distribution function with thermal velocity V_i .

Since $\rho_e < L_E$, the electric field given in Eq. (1) causes a cross-field electron flow in the y direction. Because the electric field is nonuniform, the distribution function deviates from being a simple drifting Maxwellian [7]. Expansion in terms of the assumed small parameter ρ_e / L_E leads to the following result:

$$F_e = \frac{n_e(X_g)}{[\eta(x)]^{1/2}(\pi V_e)^{3/2}} \exp\left\{-\frac{w_\perp^2 + v_z^2}{V_e^2}\right\},$$

where $X_g = x + v_y/\Omega_e$ is the guiding center, Ω_e is the electron cyclotron frequency, $w_\perp^2 = v_x^2 + w_y^2/\eta(x)$, $w_y = v_y - V_E(x)$, $V_E(x) = -E(x)/B_0$ is the sheared electron cross-field flow, V_e is the electron thermal velocity, and $\eta(x) = 1 + V_E'/\Omega_e$. The expression is accurate to second order in ρ_e/L_E , and we use a prime to denote taking the derivative with respect to x . Finally, to initialize the system, the electron density is determined from the quasineutrality condition $n_e(x) = n_i(x) - (1/e)E'$, where e is the electron charge.

The nonlinear evolution of the system is investigated using a standard, electrostatic, $2\frac{1}{2}$ D particle-in-cell (PIC) code in which the ions respond to the full Lorentz force, i.e., they are not assumed to be unmagnetized. The values of the physical parameters used in the simulation are $L_x/\lambda_D = 41.6$, $L_y/\lambda_D = 100$, $L_E/\lambda_D = 1.6$, $x_0/L_E = 6.4$, and $\rho_e/\lambda_D = \omega_{pe}/\Omega_e = 0.52$. The quantities L_x and L_y denote the system length in the x and y directions, respectively, ω_{pe} is the electron plasma frequency corresponding to the region of higher plasma density, and $\lambda_D = V_e/\omega_{pe}$ is the Debye length. The ion to electron mass ratio being used is 400, the ion and electron temperatures are equal to each other, and the total number of particles used in the simulation is 786432, half of which are ions and half electrons.

The electric field is decomposed into two constituents: The first is doubly periodic in the two spatial dimensions, and the second is time independent and given by Eq. (1). This latter component represents the effects of a constant driver in the system. For instance, in the case of magnetospheric boundary layers, it models the effects due to coupling with the solar wind, which maintains density variations of over 2 orders of magnitude in a distance smaller than, or of the order of, the ion Larmor radius at the boundary layers [1]. The time-dependent doubly periodic field component is obtained by solving Poisson's equation in a mesh containing 64 nodes in the x direction and 128 nodes in the y direction.

We next demonstrate that whenever the dimensionless quantity $\kappa = \omega_S/\omega_{LH}$ is larger than unity, the EIH mode is excited [6] and dominates the nonlinear evolution of the ensuing lower hybrid waves. To see the physical origin of this effect, consider the linear dispersion relation for the electrostatic potential $\psi(x)$ of lower hybrid waves. Assuming a flutelike perturbation, there results the following approximate equation for $\psi(x)$ [6]:

$$\begin{aligned} \frac{d}{dx} \left[A(x) \frac{d\psi(x)}{dx} \right] - k_y^2 A(x) \psi(x) \\ = \delta^2 \left(\frac{k_y \Omega_e}{\omega - k_y V_E} \right) S_e \psi(x), \quad (2) \end{aligned}$$

where the perturbation has been Fourier decomposed

with ω the angular frequency and k_y the wave number in the y direction. In addition, $A(x) = (1 + \delta^2)(1 - \omega_{LH}^2/\omega^2)$, $\delta = \omega_{pe}/\Omega_e$, and $S_e = (\ln n_e)' - V_E''/\Omega_e$. If shear effects are neglected and the local approximation is employed in Eq. (2), the well-known dispersion relation for the lower hybrid drift instability is recovered [4]. However, if the flow is such that $\omega_S > \omega_{LH}$ (i.e., $\kappa > 1$), the resonance condition $\omega - k_y V_E \sim 0$ is satisfied within the flow channel leading to substantial changes in the wave dispersion properties: The EIH mode is excited with a characteristic wavelength which we have found to be comparable to L_E (i.e., $k_y L_E \sim 1$) [6]. Since the EIH instability is a resonant fluidlike mode, it is similar in character to the Kelvin-Helmholtz instability [8], its principal difference with this mode being the additional resonance $(1 - \omega_{LH}^2/\omega^2)$ appearing in the coefficient $A(x)$. We conclude that $\kappa > 1$ is the condition to be satisfied in order for shear in the electron cross-field flow to play an important role in the time evolution of nonlinear lower hybrid instabilities. A similar result (i.e., that shear plays an important role when $\kappa > 1$) was recently obtained in a study which examined the linear theory of nonlocal effects on the lower hybrid drift instability [9].

The two spatial variables on which the plasma quantities depend are x and y . For the magnetic field being directed along the z axis, this corresponds to flute perturbations, i.e., $k_\parallel = 0$. For reference, $t = 0$ corresponds to the system being in equilibrium. In order to best illustrate the principal conclusions of this paper, we choose an electric field amplitude such that $\omega_S = E_0/B_0 L_E = 10.8\omega_{LH}$ (i.e., $\kappa = 10.8$). We present in Fig. 1 a contour plot of the electrostatic potential $\Phi(x, y)$ which clearly shows the formation of closed potential contours

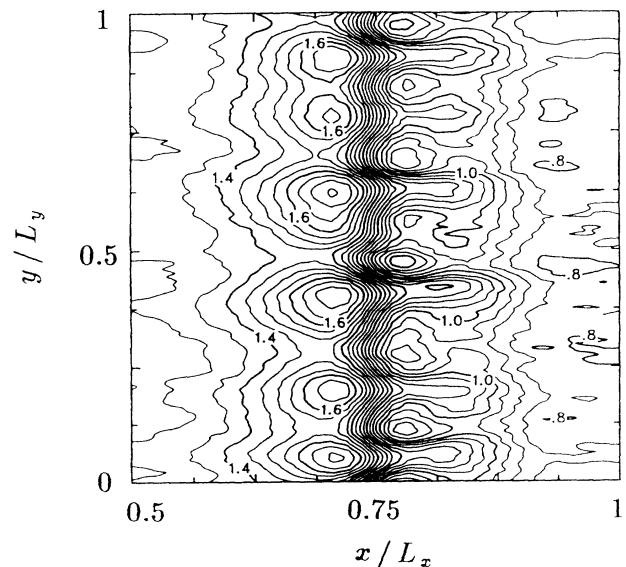


FIG. 1. Contour plot of the electrostatic potential showing the formation of coherent vortex structures at $\omega_{LH}t = 7.2$. The sheared flow has been chosen so that $\kappa = 10.8$.

after a time interval corresponding to $\omega_{LH}t = 7.2$. Since the electron motion occurs (approximately) on surfaces of constant electric potential, these structures imply the generation of coherent vortex structures in the plasma flow. As these coherent structures evolve, they tilt with respect to the x axis making (alternatively) an angle of the order of $\pm 15^\circ$. This observation is common to a number of nonlinear simulations of shear-driven instabilities in fluid mechanics [10].

There are three important features associated with the formation of these coherent structures. First, we find that the structures typically last for 20 lower hybrid times, somewhat over 2 ion gyroperiods. The reason for this is that the system exhibits substantial anomalous viscosity: For $\kappa > 5$, the magnitude of the cross-field flow is found to diminish as a function of time according to $1/\sqrt{1+Kt}$, where K depends on κ but is time independent. Hence, the source of free energy for the instability is rapidly depleted and this accounts for the typical lifetime of these coherent structures. In conjunction with the decay of the vortexlike structures, the typical frequency of the system cascades down toward the ion cyclotron frequency. Second, we find that as κ is varied (by changing the value of E_0 while keeping all other parameters fixed), the wavelength of these structures is closely correlated with that of the fastest growing mode obtained by solving the linear dispersion relation of the EIH instability [6]. This is shown in Table I, which indicates that for $\kappa > 1$ the typical wavelength of the shear-driven lower hybrid waves satisfies the relation $k_y L_E \sim 0.7$. Note that in view of the condition $\rho_e < L_E$, the EIH wavelength is much longer than the one corresponding to the lower hybrid drift instability, for which $k_y \rho_e \sim (T_e/T_i)^{1/2}$, where T_e is the electron temperature. Table I also indicates that the wavelength becomes larger as the value of κ is increased while keeping $T_e/T_i = 1$. More importantly, we find that for $\kappa < 1$, the time evolution of the system is such that the potential $\Phi(x, y)$ no longer develops closed potential contours (by inference, vortex structures in the plasma flow). Rather, it exhibits lateral kinks whose characteris-

tic wavelength is on the order of the electron Larmor radius. These latter features have been previously observed in the nonlinear evolution of the lower hybrid drift instability [4], and imply that a smooth transition takes place in the system dynamics depending on whether κ is larger or smaller than unity, velocity shear effects dominating when $\kappa > 1$. Third, we find that the development of these coherent structures is not hindered if the magnetic field is allowed to make a small but finite angle with the z axis (i.e., by a finite but small value of k_{\parallel}). For example, for $\kappa = 10.8$, the magnetic field can make an angle of up to 10° with the z axis before the formation of these structures is appreciably diminished.

Figure 2 shows the y velocity ion distribution function, both at equilibrium ($t = 0$) and at time $\omega_{LH}t = 20.3$, for $\kappa = 10.8$. The distribution function is calculated using only those ions which are present at the given times in the immediate vicinity of the sheared electron flow channel (a subset of the simulation box within which small fluctuations occur in the local ion density): To be specific, within the domain $\Delta < 3.2$ and $|(y - L_y/2)/L_E| < 3.8$, where $\Delta = |(x - L_x/2 - x_0)/L_E|$. For the long-wavelength mode considered in this study, ion acceleration can result from the resonant interaction of ions with a time-varying electric field directed along the y axis, i.e., we need not invoke three-wave coupling processes [11] to develop low-phase-velocity waves in the system. To see this, note that the y velocity for resonant ion interaction is given by $v_r = \mu V_i(\omega_{LH}/\omega_{pi})(L_E/\lambda_D)/k_y L_E$, where $\mu = Z_i T_e/T_i$, Z_i is the ion charge state, and ω_{pi} is the ion plasma frequency. For the case $\kappa = 10.8$, we find that $v_r \sim 2V_i$, which correlates well with the result shown in Fig. 2.

In this Letter, we have reported the occurrence of coherent structures (vortexlike) and significant resonant ion acceleration in the nonlinear evolution of lower hybrid instabilities. These effects have been shown to be gen-

TABLE I. Comparison between the wavelength corresponding to the fastest growth rate of the EIH mode (given under the heading $k_y L_E$) and the resulting number of vortices (V) or kinks (K) observed in the PIC simulation (given under the heading N PIC). The number of vortices corresponding to the EIH mode wavelength is shown under the heading N EIH. The definition $\alpha_e = \omega_S/\Omega_e$ is used.

α_e	κ	$k_y L_E$	N EIH	N PIC	V/K
0.25	10.8	0.40	4	6	V
0.20	8.7	0.50	5	7	V
0.15	6.5	0.60	6	8	V
0.10	4.3	0.80	8	10	V
0.05	2.2	1.25	12	11	V, K
0.01	0.4	3.30	40	14	K

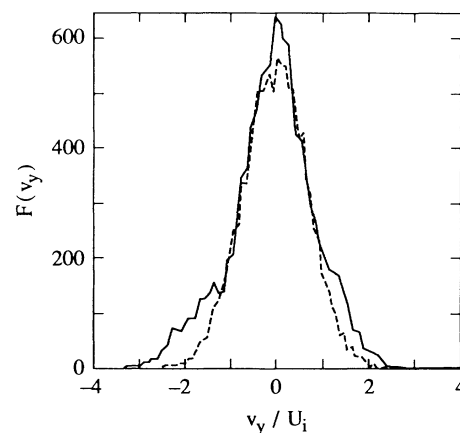


FIG. 2. The ion distribution function, given at equilibrium (dashed curve) and at time $\omega_{LH}t = 20.3$ (solid curve), shows resonant ion acceleration due to the long-wavelength shear-driven ($\kappa = 10.8$) lower hybrid turbulence.

erated by the presence of sufficient shear ($\kappa > 1$) in an electron cross-field flow. The conclusions of this work significantly impact the following areas: (i) space plasma physics, in particular, shocklike and magnetospheric boundary layer dynamics, (ii) the physics of laser-produced plasma jets, and (iii) research on chemical release experiments in the Earth's magnetotail. This work is particularly pertinent in the study of magnetospheric boundary layer dynamics on account of recent observational evidence which establishes that sharp density gradients exist in such structures [1]. In regard to laser-produced plasma jets, we note that the wavelength and growth rates observed in their structuring have been recently shown to be well described by the EIH mode discussed in this study [2]. Finally, in connection with chemical release experiments [3], we note that the lower hybrid drift instability has thus far been the leading candidate used to explain the structuring of the barium plasma clouds released in the Earth's magnetotail [12]. However, the wavelength associated with this instability has been found to be up to 10 times smaller than that typically observed. Since significant shear develops in the electron cross-field flow of the expanding barium clouds [3], we propose that the electron-ion-hybrid mode presented in this study is a likely candidate to account for the experimental observations.

This research was supported by the Office of Naval Research and the National Aeronautics and Space Administration. One of the authors (H.R.) was an Office of Naval Technology Postdoctoral fellow during the course of this work.

[1] H. Romero, G. Ganguli, P. Palmadesso, and P. B. Dusen-

- bery, *Geophys. Res. Lett.* **17**, 2313 (1990); P. Song, R. C. Elphic, C. T. Russell, J. T. Gosling, and C. A. Cattell, *J. Geophys. Res.* **95**, 6375 (1990); G. K. Parks, M. McCarthy, R. J. Fitzenreiter, J. Etcheto, K. A. Anderson, R. R. Anderson, T. E. Eastman, L. A. Frank, D. A. Gurnett, C. Huang, R. P. Lin, A. T. Y. Lui, K. W. Ogilvie, A. Pedersen, H. Reme, and D. J. Williams, *J. Geophys. Res.* **89**, 8885 (1984).
- [2] A. N. Mostovych, B. H. Ripin, and J. A. Stamper, *Phys. Rev. Lett.* **62**, 2837 (1989); T. A. Peyser, C. K. Manka, B. H. Ripin, and G. Ganguli, *Phys. Fluids B* **4**, 2448 (1992).
- [3] P. A. Bernhardt, R. A. Roussel-Dupre, M. B. Pongratz, G. Haerendel, A. Valenzuela, D. A. Gurnett, and R. R. Anderson, *J. Geophys. Res.* **92**, 5777 (1987).
- [4] N. A. Krall and P. C. Liewer, *Phys. Rev. A* **4**, 2094 (1971); D. Winske and P. C. Liewer, *Phys. Fluids* **21**, 1017 (1978); Y.-J. Chen, W. M. Nevins, and C. K. Birdsall, *Phys. Fluids* **26**, 2501 (1983).
- [5] J. B. McBride, E. Ott, J. P. Boris, and J. H. Orens, *Phys. Fluids* **15**, 2367 (1972).
- [6] G. Ganguli, Y. C. Lee, and P. J. Palmadesso, *Phys. Fluids* **31**, 2753 (1988); H. Romero, G. Ganguli, Y. C. Lee, and P. J. Palmadesso, *Phys. Fluids B* **4**, 1708 (1992).
- [7] G. Ganguli, Y. C. Lee, and P. J. Palmadesso, *Phys. Fluids* **31**, 823 (1988).
- [8] P. G. Drazin and L. N. Howard, in *Advances in Applied Mechanics* (Academic, New York, 1966), Vol. 9, Chap. 1.
- [9] N. T. Gladd and S. H. Brecht, *Phys. Fluids B* **3**, 3232 (1991).
- [10] N. J. Zabusky and G. S. Deem, *J. Fluid Mech.* **47**, 353 (1971); A. Miura and T. Sato, *J. Fluid Mech.* **86**, 33 (1978).
- [11] J. M. Retterer, T. Chang, and J. R. Jasperse, *J. Geophys. Res.* **91**, 1609 (1986).
- [12] For an overview of the subject, see, for example, D. Winske, *Phys. Fluids B* **1**, 1900 (1989), and references therein.